

under consideration are not included. In the case of PVN, 1,3-dinaphthylpropane, or 2-methylnaphthalene with the DCNB acceptor, it has been concluded that the exterplex is formed from attack of a naphthalene donor D on the naphthalene–DCNB(D^+-A^-)^{*} exciplex. Such a mechanism seems quite reasonable since attack of the highly polar exciplex ($\mu_e > 10$ D) by an electron donor would stabilize the complex by distributing the positive charge over two naphthalene chromophores. An attack of the nonpolar excimer could result in the exciplex or the exterplex. If the exciplex were formed, it would be highly susceptible to attack by the neighboring naphthalene partner of the original naphthalene–naphthalene excimer. It is difficult to suggest this same mechanism for the PVCz–DMTP system from the time-resolved spectra given in Figure 1. It may be that the pathway proceeding through the polar exciplex is the major pathway for exterplex formation. However, direct formation of the exterplex by attack of the carbazole sandwich excimer by DMTP cannot be excluded. In both cases, the stability of the exterplex is provided by the distribution of the positive charge over the two donor chromophores.

It appears that the polymer chain provides an excellent structure for holding a second aromatic chromophore in the position required for the exterplex formation since these do not form in simple small-molecule models. Furthermore, the unique separation of charge which occurs in the PVN–DCNB or PVCz–DMTP systems may be simple analogues for the process of charge separation in photosynthesis.¹² Also, it may be possible to quench the exterplex emission effectively. This would provide a mechanism for transfer of electron density from an electron donor to the electron acceptor (DMTP) separated by the

two carbazole chromophores and the polymer. Such electron-transfer reactions could be of some importance in natural or synthetic photochemical energy conversion schemes.

Acknowledgment. The authors wish to acknowledge the generous financial support of this work by the National Research Council of Canada.

References and Notes

- (1) Address correspondence to this author.
- (2) F. D. Lewis and C. E. Hoyle, *J. Am. Chem. Soc.*, **97**, 5950 (1975); **98**, 4338 (1976); **99**, 3779 (1977); D. Rehm and A. Weller, *Isr. J. Chem.*, **8**, 259 (1970); N. E. Schore and N. J. Turro, *J. Am. Chem. Soc.*, **97**, 2482 (1975); D. A. Labianca, G. N. Taylor, and G. S. Hammond, *ibid.*, **94**, 3679 (1972); M. Gordon and W. R. Ware, Ed., "The Exciplex", Academic Press, New York, 1975.
- (3) R. A. Caldwell, D. Creed, and H. Ohta, *J. Am. Chem. Soc.*, **96**, 2994 (1974); D. Creed and R. A. Caldwell, *ibid.*, **96**, 7369 (1974); H. Ohta, D. Creed, P. H. Wine, R. A. Caldwell, and L. A. Melton, *ibid.*, **98**, 2002 (1976).
- (4) T. Mimura and M. Itoh, *J. Am. Chem. Soc.*, **98**, 1095 (1976).
- (5) W. Klöpffer, "Intermolecular Excimers in Organic Molecular Photochemistry", J. B. Birks, Ed., Wiley-Interscience, New York, 1973, p. 357.
- (6) M. T. Vala, J. Haebig, and S. A. Rice, *J. Chem. Phys.*, **43**, 886 (1965).
- (7) G. E. Johnson, *J. Chem. Phys.*, **62**, 4697 (1975).
- (8) A. Itaya, K. Okamoto, and S. Kusabayashi, *Bull. Chem. Soc. Jpn.*, **49**, 2082 (1976); G. Pfister, D. J. Williams, and G. E. Johnson, *J. Phys. Chem.*, **78**, 2009 (1974); K. Okamoto, S. Kusabayashi, and H. Mikawa, *Bull. Chem. Soc. Jpn.*, **46**, 2613 (1973).
- (9) C. E. Hoyle, T. L. Nemzek, A. Mar, and J. E. Guillet, *Macromolecules*, **11**, 429 (1978).
- (10) C. E. Hoyle and J. E. Guillet, *Macromolecules*, **11**, 221 (1978).
- (11) S. Georgiou, *Nature (London)*, **259**, 423 (1976).
- (12) R. A. White and G. Tollin, *Photochem. Photobiol.*, **14**, 43 (1971); J. R. Harbour and G. Tollin, *ibid.*, **20**, 271 (1974).

Melt Rheology of Four-Arm and Six-Arm Star Polystyrenes

W. W. Graessley and J. Roovers*

Department of Chemical Engineering and the Department of Materials Science, Northwestern University, Evanston, Illinois 60201, and the National Research Council of Canada, Ottawa, Ontario, Canada, K1A 0R9.[‡] Received March 28, 1979

ABSTRACT: The dynamic moduli of linear, four-arm and six-arm star polystyrene melts were measured over a wide range of frequencies and temperatures by the eccentric rotating disk method. The zero-shear viscosities of the star polystyrenes were less than those linear polystyrenes of the same molecular weight ($M < 10^6$). However, viscosities of the high molecular weight stars were larger when comparisons were made at a constant radius of gyration. The observed enhancements agree with those found in polybutadiene stars when compared on the basis of the parameter $Z(M_w/M_e)$, where Z and M_e are constants characteristic of each polymer, and M_w is the molecular weight of the arm. The zero-shear recoverable compliance of the star polymers is well-described by the Rouse–Ham formula $J_e^0 = 0.4g_2\rho RT/M$. The plateau modulus G_N^0 appears to be the same for linear and star polystyrenes. The frequency dependence of the dynamic moduli was examined for the possible presence of a second relaxation mechanism in high molecular weight stars, giving rise to viscosity enhancement, which is absent in the terminal spectrum of linear polymers.

The steady flow properties of polymer melts are usually characterized by viscosity and recoverable shear compliance. At sufficiently low shear rates (the zero-shear limit), both material properties become constants, η_0 and J_e^0 . Studies of zero-shear viscosity in numerous linear random-coil polymers of narrow molecular weight dis-

tribution have now clearly established two regions. For low molecular weight polymers, η_0 is directly proportional to molecular weight M ; for high molecular weight polymers, η_0 is proportional to $M^{3.4}$. A molecular weight characteristic of the polymer, M_c , separates the two regions.^{1–3} Two regions have also been established for the zero-shear recoverable compliance. At low molecular weights, J_e^0 is directly proportional to M ; at high molecular weights, J_e^0 is independent of molecular weight. A second characteristic molecular weight, M_c' , separates the two regions.³

* Address correspondence to this author at the National Research Council of Canada.

[‡] Issued as NRCC No. 17649.

The experimental observations for low molecular weight samples are understood at the molecular level as being due to the largely independent motions of chains, describable in terms of the Rouse model.⁴ At high molecular weights, the motions are assumed to be coupled, the coupling being visualized and interpreted in terms of chain entanglements.^{2,3}

The experimental melt rheology of polymers with long branches is less well established. Predictions based on extensions of the linear polymer theories to branched polymers^{5,6} suggest that both η_0 and J_e^0 should be smaller for branched polymers and that η_0 for linear and branched polymers should be the same at the same radius of gyration. The predictions for η_0 are confirmed experimentally for polystyrene, polyisoprene, and poly(α -methylstyrene) stars in solutions of low and moderate concentration.⁷⁻⁹ Melt viscosities of polystyrene stars are also lower than those of linear polystyrenes.^{10,11} However, in 1965 Kraus and Gruver showed that the predicted reduction in melt viscosity is observed only at low molecular weights in three-arm and four-arm polybutadiene stars. At high molecular weights, the viscosities of the stars were many times larger than those of their linear counterparts.¹² In their 1968 review, Berry and Fox concluded that the viscosity enhancement in stars depends exponentially on the number of entanglements along the arms.¹ An extensive study of the molecular weight and concentration dependence of viscosity for polyisoprene stars supports the exponential form,¹³ and recent theory provides some additional justification.¹⁴

The situation is somewhat similar in the case of recoverable compliance. The theoretical reduction of J_e^0 for stars relative to linear polymers is observed only at low concentrations and molecular weights.^{13,15} Values of J_e^0 for star polystyrene melts are reported to be about 1.5×10^{-5} cm²/dyn,¹¹ larger than the limiting value for linear polystyrenes by approximately a factor of 10. Crossovers between reduction and enhancement with respect to concentration and molecular weight were found in solutions of polyisoprene stars.¹³ The present study was undertaken to establish more clearly the factors controlling enhancement of η_0 and J_e^0 in star polymers. Other features of the frequency dependence of the dynamic moduli were also investigated and compared.

Experimental Section

The preparation, fractionation, and characterization of the four- and six-branch star polystyrenes (series S and H, respectively) were reported previously.¹⁵ The narrow molecular weight distribution of the samples was established by number- and weight-average molecular weight determinations and ultracentrifugation sedimentation. Two linear samples, similarly well characterized, are included for comparison. GPC curves showed that no change had occurred in the samples since their synthesis. Concentrated solution properties of the stars were reported previously.^{7,16}

Dynamic moduli were obtained on the undiluted melts with a Rheometrics Mechanical Spectrometer in the eccentric rotating disk (ERD) mode. The steady-state storage modulus G' and loss modulus G'' were obtained as functions of frequency ω from measurements of steady-state forces by procedures described elsewhere.¹⁷ The frequency range of the instrument is from 10^{-3} to 10^2 radians/s. The platen radius was 1.25 cm, and the platen separation was between 0.10 and 0.12 cm. The measurements were performed in the linear regime by using a small eccentricity and reducing it for high-frequency measurements. Linearity was confirmed repeatedly by measurement with different eccentricities. The eccentricity was corrected for instrumental compliance using 3.44×10^{-9} cm/dyn for the compliance constant.^{17,18} The 10% uncertainty associated with this constant¹⁸ would only slightly affect moduli of the order of 10^6 dyn/cm² and less.

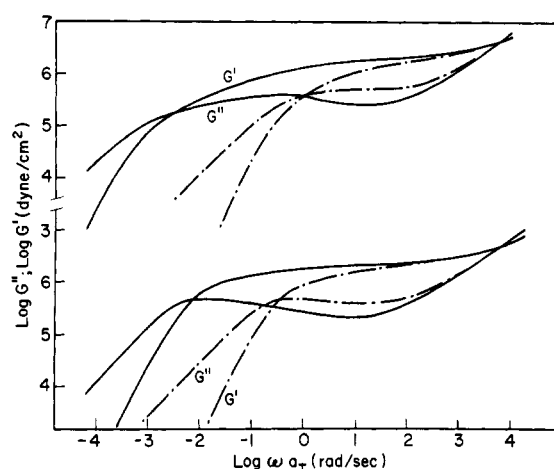


Figure 1. Storage and loss moduli-frequency curves. Top: full line, S181A; broken line, S161A. Bottom: full line, C7bb; broken line, C6bb. Numerical data on all samples are available on request from the authors or from CISTI, NRCC, Ottawa, Ontario, Canada.

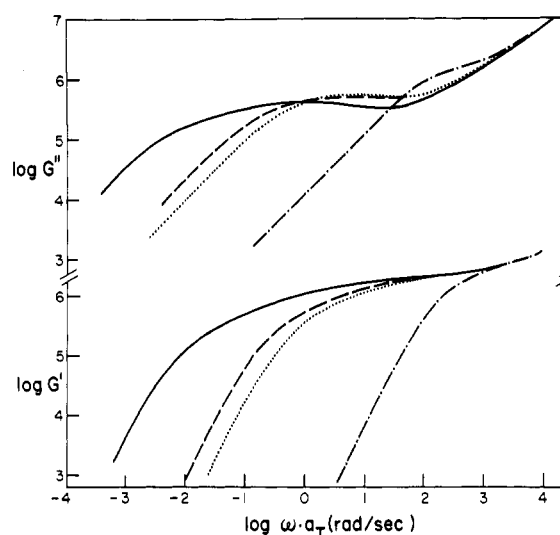


Figure 2. Moduli-frequency curves for six-arm stars at 169.5 °C: full line, HSO51A; broken line, HS111A; dotted line, HSO41A; chain line, HSO61A.

The polystyrene powders were mixed with 0.2% Santonox and vacuum molded at 160 °C into clear, bubble-free disks. Measurements were made between 140 and 200 °C; the highest temperature used depended on the sample molecular weight. The thermostated chamber was flushed continuously with high-purity nitrogen. Under these conditions, sample degradation became a problem only when the sample was held above 190 °C for more than a few hours. Repeat measurements at a low frequency were used to check for sample degradation. Agreement within 5% was required for acceptance of data to calculate G' and G'' .

Results

Typical examples of the storage and loss moduli as functions of frequency for star-branched polymers are compared with those of a linear polystyrene in Figure 1. Master curves were obtained from measurements at different temperatures and superimposed to the data at 169.5 °C by experimental shift factors (a_T) along the frequency axis. No vertical shifts seem to be required in the small-temperature range used. Moduli-frequency curves for the six-arm star polymers are shown in Figure 2.

For the linear polystyrenes, the shift factors can be represented by a Vogel equation²

$$\log a_T = \frac{A}{2.303} + \frac{B}{2.303(T - T_\infty)} \quad (1)$$

Table I
Viscoelastic Parameters for Polystyrenes at a Reference Temperature of 169.5 °C and
Corrected to Constant Segmental Friction

sample	$M_w \times 10^{-5}$	$[\eta]_0$	$\eta_0 \times 10^{-6}$	$J_e^0, \text{cm}^2/\text{dyn}$ ($\times 10^6$)	$\log G''_{\max}$	$G_N^0, \text{dyn}/\text{cm}^2$ ($\times 10^{-6}$)	Γ
linear							
PS100f2	1.15	0.308	0.167 ^a	1.08	5.71		
C6bb	2.75	0.440	3.1	1.20	5.70	2.06	
C7bb	8.60	0.779	150	1.25	5.70	2.11	
four star							
S121A	0.935	0.191	0.0183	0.6		>1.64	
S161A	3.51	0.384	1.14	1.9 (2.0)	5.70	1.77	0.93
S141AB	5.21	0.448	6.7	2.4	5.65	1.96	1.91
S221A	8.97	0.589	83	4.6	5.60	1.82	3.7
S181A	10.27	0.635	230	5.8 (6.0)	5.60	2.04	6.1
S171A	13.0						
six star							
HS061A	1.10	0.177	0.0115	0.43		1.78	
HS041A	5.09	0.374	0.995	1.8	5.72	1.83	0.97
HS111A	5.91	0.405	2.15	2.0	5.72	2.01	1.22
HS051A	10.9	0.557	35.7	3.8	5.63	1.96	2.32

^a Measured by Dr. G. Marin at 160.0 °C and shifted to 169.5 °C.

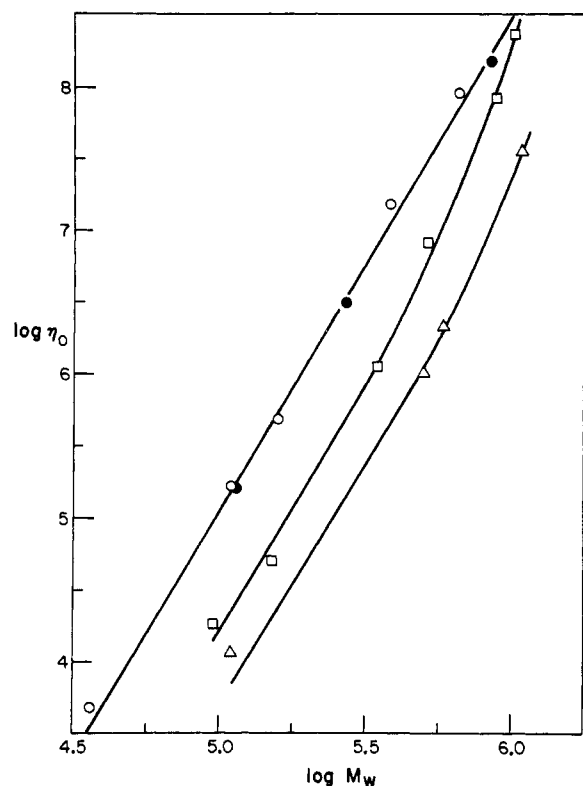


Figure 3. Zero-shear viscosity at 169.5 °C vs. molecular weight: full circles, linear polymer, this work; open circles, linear polymer, ref 21; squares, four-arm stars; triangles, six-arm stars.

with $B = 710$ and $T_\infty = 49$ °C. No great precision is claimed for these constants in view of the limited experimental range in temperature and molecular weight. The same constants represent the experimental shift factors for the star polymers. The two low molecular weight star polystyrenes, S121A and HS061A, have glass-transition temperatures respectively 2.3 and 2.9 °C lower than high molecular weight linear polystyrene.¹⁹ When T_∞ is lowered by these amounts, the coefficient $B/2.303$ is experimentally indistinguishable from those of high molecular weight polystyrene. The moduli were reduced to constant friction factor conditions.¹ Similarly, because sample S161A contains 0.9 wt % isoprene, it has a T_g 3 °C lower than high molecular weight polystyrene.²⁰ The experimental moduli of this sample were also cor-

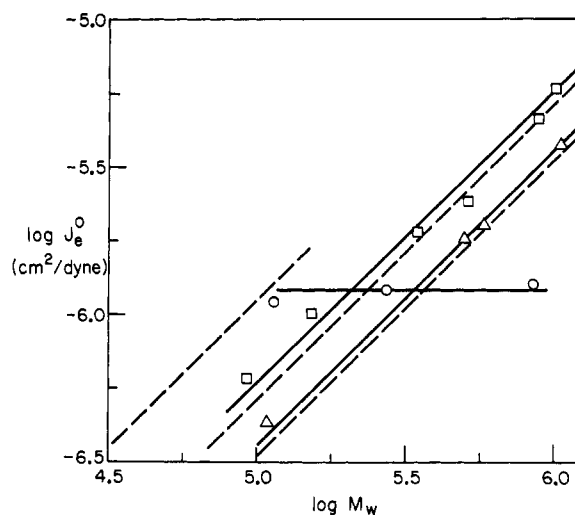


Figure 4. Zero-shear recoverable compliance vs. molecular weight: circles, linear polymer; squares, four-arm stars; triangles, six-arm stars; dotted lines, eq 9.

rected to a constant friction factor.

At low frequencies, the experimental loss moduli depend linearly on the frequency. The zero-shear viscosities of all samples were obtained from²

$$\eta_0 = \lim_{\omega \rightarrow 0} \frac{G''(\omega)}{\omega} \quad (2)$$

These data, reduced to 169.5 °C, are collected in Table I.

The molecular weight and polymer structure dependence of the zero-shear melt viscosities are shown in Figure 3. All polymers studied show the plateau in $G'(\omega)$ characteristic of entangled molecules. All star-branched polystyrenes investigated have zero-shear viscosities $(\eta_0)_B$ lower than $(\eta_0)_L$ for linear polymer of the same molecular weight. However, the ratio $(\eta_0)_B/(\eta_0)_L$ is not constant and in fact approaches unity for the four-star polystyrene of highest molecular weight.

The experimental storage moduli at low frequencies depend on the square of the frequency. Accordingly, zero-shear recoverable compliances were obtained from²

$$J_e^0 = \frac{1}{\eta_0^2} \lim_{\omega \rightarrow 0} \frac{G'(\omega)}{\omega^2} \quad (3)$$

The results are collected in Table I and plotted in Figure 4. While J_e^0 for linear narrow molecular weight distri-

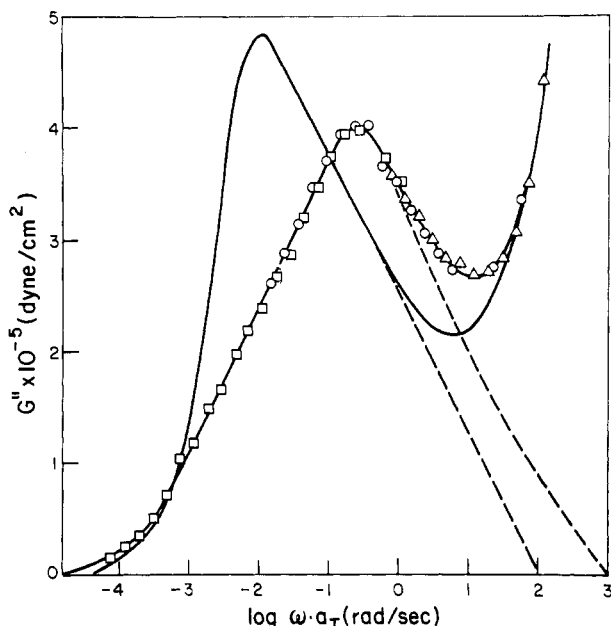


Figure 5. Loss moduli vs. $\log \omega$ used to determine the plateau modulus G_N^0 according to eq 5: full line, C7bb; line with experimental points, S181A; triangles, 155 °C; circles, 170 °C; squares, 200 °C; broken line, extrapolation of the plateau contribution.

bution polystyrene melts reach a limiting value of $1.2\text{--}1.3 \times 10^6 \text{ cm}^2/\text{dyn}$ when $M_w > M_c' = 1.3 \times 10^5$,³ the values for the star polystyrenes show a first-order dependence over the whole range of molecular weights investigated. At low M_w , J_e^0 of the star polymers is smaller than that of the linear polymers, but at high M_w it becomes larger.

Because the storage modulus at intermediate frequencies (in the plateau region) does not become truly constant, the plateau modulus was estimated from the area under the terminal loss peak²

$$G_N^0 = \frac{2}{\pi} \int_{-\infty}^{+\infty} [G''(\omega) - G_s''(\omega)] d \ln \omega \quad (4)$$

Contributions from the transition zone (G_s'') ($\omega > 1 \text{ s}^{-1}$ at 169.5 °C) were estimated from the data of the linear polystyrenes. In high molecular weight linear polystyrenes, the terminal and transition regions are well separated. However, star polystyrenes have a broader maximum in G'' at frequencies somewhat nearer the transition region (see Figure 5). As a result, G_N^0 for the stars has a larger uncertainty, especially for those of lower molecular weight. The values of G_N^0 obtained are given in Table I.

The frequency dependence of the moduli of star and linear polymers is considerably different as can be seen from Figure 1. In linear polystyrene, the crossover of G' and G'' values in the terminal region almost coincides with the maximum in G'' , corresponding to the typical isolated band of relaxation times for narrow molecular weight distribution polymers.^{2,3} In the star polystyrenes, even in cases where the zero-shear viscosity is not enhanced (S161A, HSO41A), the crossover of G' and G'' occurs at a lower frequency than the maximum in G'' , suggesting a broader terminal relaxation spectrum. The crossover of G' and G'' moves to lower frequencies and further from the maximum in G'' as the molecular weight of the arms increases. Also, in these cases, the value of G''_{max} becomes lower than that for linear polymers. (See Figure 5 and Table I.)

Discussion

The zero-shear viscosities of the linear polystyrenes at 169.5 °C reported here are well represented by $\log \eta_0 =$

$-12.01 + 3.40 \log M_w$, in excellent agreement with earlier data obtained on Pressure Chemical polystyrene samples²¹ and other published data obtained with a variety of other experimental techniques.²²⁻²⁶ The zero-shear compliance of the high molecular weight linear sample ($M_w = 860\,000$) is considerably lower than that observed for the Pressure Chemicals polystyrene of the same molecular weight.²⁵⁻²⁷ This is presumed to reflect the lower polydispersity of our homemade polystyrene.

Two factors are considered in comparing viscosities of star and linear polymers of the same molecular weight. One describes an expected reduction of η_0 due to the smaller radius of gyration and branched polymers. The other deals with the enhancement of η_0 found to exist in high molecular weight branched polymers.

On theoretical grounds,^{1,6} the reduction follows from the expected dependence of viscosity on radius of gyration rather than molecular weight, per se. That is,

$$\eta_0 = K(\langle s^2 \rangle_\theta)^a = K'([\eta]_\theta)^a \quad (5)$$

where $\langle s^2 \rangle_\theta$ is the unperturbed radius of gyration of the polymer, $[\eta]_\theta$ is intrinsic viscosity in a θ solvent, and $a = 1$ or 3.4 for polymers with $\langle s^2 \rangle_\theta$ below or above that corresponding to the characteristic molecular weight M_c for linear polymers. For star polymers

$$\left(\frac{\langle s^2 \rangle_{\theta, \text{star}}}{\langle s^2 \rangle_{\theta, \text{lin}}} \right)_M = g = \frac{3f - 2}{f^2} \quad (6)$$

with f the number of arms in the star. The second part of eq 5 follows from $[\eta]_\theta \propto M^{1/2}$ and $\langle s^2 \rangle_\theta \propto M$. For branched polymers, it is only identical with the first part provided $g_\theta' = g^{1/2} = ([\eta]_{\theta, \text{star}}/[\eta]_{\theta, \text{lin}})_M$. There is ample experimental evidence that eq 5 and 6 describe the reduction of η_0 of star polymers in solution where enhancement effects are minimized or absent^{7-9,13} and in melts of low molecular weight polymers.^{10,12} Since $g_\theta' = g^{0.58}$ for the star polymers used here,^{8,16} superposition of zero-shear viscosity data at constant $\langle s^2 \rangle_\theta$ or constant $[\eta]_\theta$ differs slightly. The present melt viscosities for star polystyrenes are plotted against $[\eta]_\theta^2$ in Figure 6.

Figure 6 clearly shows an enhancement of η_0 in the star polymers at high molecular weights. The enhancement factors in Table I are calculated from

$$\Gamma = (\eta_0)_{\text{obsd}}/(\eta_0)_{\text{calcd}} \quad (7)$$

with $\log (\eta_0)_{\text{calcd}} = 8.915 + 3.40 \log [\eta]_\theta^2$. Similar enhancement factors were observed in star-branched polybutadiene melts and in concentrated solutions of star-branched polyisoprenes^{12,13} but not in four-arm star polystyrenes.^{10,11}

The enhancement of η_0 found for branched polymers is thought to be caused by the slowing of the reptation along a backbone contour when long arms are present.^{13,14} Configurational renewal times for stars increase exponentially with the number of entanglements along the arm.¹⁴ Geometrical considerations of the lattice of obstructions in which a branch has to reorganize suggests that Γ should in fact be a function of the combination $(\Phi^{11/6} M_{br}/M_e)Z^{13}$ where Φ is the volume fraction of polymer, M_e is the molecular weight between entanglements in the undiluted polymer, M_{br} is the molecular weight of an arm, and Z depends on the properties of the undiluted linear species:

$$Z = 1.54 \frac{(\rho N_a)^{2/3} (\langle s^2 \rangle_\theta / M)^{1/2}}{M_e^{1/6}} \quad (8)$$

in which ρ is the density and N_a is Avogadro's number.

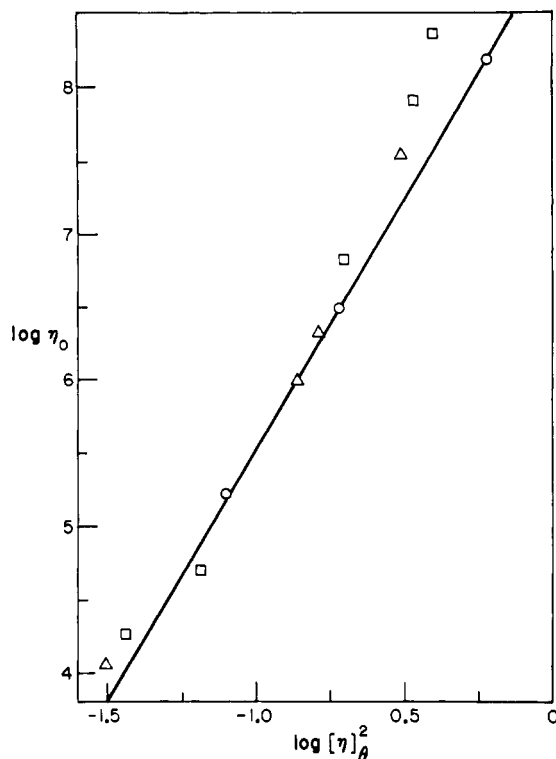


Figure 6. Zero-shear viscosity vs. the square of the Θ temperature intrinsic viscosity. Symbols as in Figure 4.

Calculated values of Z are 5.9×10^6 and 10.3×10^6 (cgs units) for polystyrene and polybutadiene, respectively.

The observed enhancement in star polystyrenes is compared with data for star polybutadienes in Figure 7. The enhancement factors of the four-arm star polymers fall near a common line, suggesting the validity of the structure factor Z . As noted with polyisoprene stars,¹³ the enhancements in four-arm and six-arm stars are little different.

From the intercept in Figure 7, it can be seen that viscosity enhancement starts to become important in star polymers when each branch participates in three or four entanglements. The enhancement observed in concentrated solutions of star polyisoprenes fit the line in Figure 7 only when $\Phi^{3/2}$ dependence of enhancement is assumed, as was suggested previously.¹³

Zero-shear recoverable compliance data for the star polystyrenes were compared with theoretical calculations based on the Rouse–Ham model^{4,5}

$$J_e^0 = 0.4g_2 \frac{M}{cRT} \quad (9)$$

in which

$$g_2 = \frac{15f - 14}{(3f - 2)^2} \quad (10)$$

Values of g_2 are 1.0, 0.46, and 0.297 for linear, four-arm, and six-arm star-branched polymers, respectively. Equation 9 is represented in Figure 4 by dotted lines. The J_e^0 values for the star polymers studied here can be calculated from theory to a remarkably good approximation. The small numerical differences may well be due to experimental errors and the neglect of small corrections for molecular weight distribution in the samples.

For linear polystyrenes in the melt, J_e^0 becomes constant at about $M_c' = 1.3 \times 10^5$.³ In star polymers, the onset of this behavior seems to be shifted to much higher molecular weights. The data obtained on 0.33 g/mL solutions of

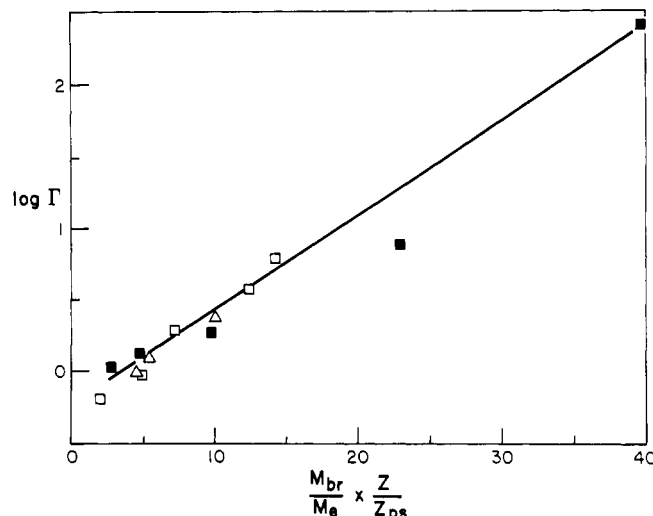


Figure 7. Enhancement of zero-shear viscosity Γ vs. number of entanglements per branch: open squares, four-arm polystyrene; open triangle, six-arm polystyrene; full squares, four-arm polybutadienes from ref 12.

four-arm star polyisoprenes suggest that J_e^0 levels off at a value about five times higher than the limiting value for linear polyisoprene.¹³ At this point, each branch of the polymer is involved in an average of six to eight entanglements. The value of J_e^0 for the highest molecular weight star polystyrene studied here is five times larger than the limiting value for linear polystyrene. No indication of leveling off is seen, but this may be because of the relatively few samples studied. It cannot be excluded, of course, that there are differences between concentrated solutions of polyisoprene and undiluted polystyrene with regard to this behavior.

The behavior of J_e^0 for the star polystyrene melts and the star polyisoprene solutions is in contrast with the constant J_e^0 observed earlier in other star polystyrene melts.¹¹ It is suggested that a combination of the structural factor and the molecular weight distribution produced J_e^0 values ten times larger than the limiting J_e^0 for linear polystyrene in those samples.

The data in Table I indicate that the plateau modulus, G_N^0 , of the star polystyrenes is constant and virtually identical with that for the linear polystyrenes. Any effects of the branch point on entanglement spacing,

$$M_e = \rho RT/G_N^0 \quad (11)$$

would be expected to be strongest in the low molecular weight samples. Unfortunately, G_N^0 values for the lowest molecular weight samples are least certain. The data, nevertheless, suggest that M_e is not strongly affected by the presence of single branch points in the molecules.

The onset of shear rate dependence of viscosity is sometimes discussed in terms of a characteristic shear rate $\dot{\gamma}_0$.³ Parallel with that treatment we will define ω_0 as the frequency at which the absolute value of complex viscosity

$$|\eta^*(\omega)| = \frac{(G'^2 + G''^2)^{1/2}}{\omega} \quad (12)$$

has decreased to 80% of the η_0 . Values of ω_0 are shown in Table II. The product $\eta_0 J_e^0 \dot{\gamma}_0$ has been found to be a constant for a wide range of polymers.³ The data given in Table II indicate that the similar product $\eta_0 J_e^0 \omega_0$ is roughly constant for linear and star polystyrene melts. (The slightly smaller values for stars and the weak trend with molecular weight we attribute to the somewhat different shapes in the $|\eta^*|$ vs. ω plots and the rather

Table II
Frequency-Dependent Properties of
Polystyrene at 169.5 °C

sample	ω_0, s^{-1}	$\eta_0 J_e^0 \omega_0$	τ_{\max}, s	$\omega_0 \tau_{\max}$
linear				
C6bb	1.9×10^{-1}	0.71	1.78	0.338
C7bb	3.8×10^{-3}	0.71	89.1	0.338
four star				
S121A	59.9	0.66	5.78×10^{-3}	0.346
S161A	2.69×10^{-1}	0.58	3.55×10^{-1}	0.0955
S141AB	3.97×10^{-2}	0.64	9.79×10^{-1}	0.0388
S221A	1.45×10^{-3}	0.55	3.38	0.0049
S181A	3.32×10^{-4}	0.44	4.46	0.0015
S171A			13.46	
six star				
HS061A	127.6	0.63	4.3×10^{-3}	0.548
HS041A	3.40×10^{-1}	0.61	2.39×10^{-1}	0.081
HS111A	1.38×10^{-1}	0.59	3.38×10^{-1}	0.047
HS051A	4.18×10^{-3}	0.57	2.23	0.009

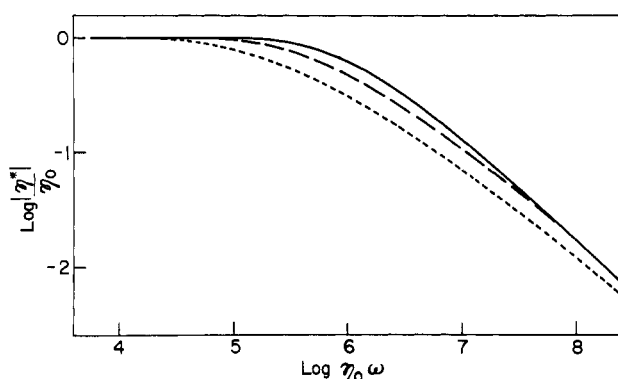


Figure 8. Frequency dependence of the reduced complex viscosity: full line, linear polystyrenes; broken line, S161A; dotted line, S181A.

arbitrary definition of ω_0). Thus, changes in η_0 and J_e^0 with molecular weight and branch structure are largely offset by compensating changes of the characteristic frequency. Similar results are obtained when ω_0 is defined in terms of the dynamic viscosity $\eta' = G''/\omega$.

For a qualitative comparison of the frequency dependence of viscosity of star polymers at low frequencies, the reduced complex viscosity ($|\eta^*|/\eta_0$) is plotted against $\omega\eta_0$ in Figure 8. This representation results in a common curve for the linear polymers, at least at frequencies where the transition zone does not interfere. In the star polymers, the curves do not overlap, and the transition from $|\eta^*| = \eta_0$ to a power-law behavior, $|\eta^*| \propto \omega^{-\alpha}$, becomes wider with increasing molecular weight.

The difference in behavior of narrow molecular weight linear and branch polymers can also be expressed in another way. The molecular weight dependence of $\tau_0 = 1/\omega_0$ follows the molecular weight dependence of η_0 . For branch polymers, the molecular weight exponent is not constant and is much stronger than the $M^{3.4}$ dependence for linear polymers. On the other hand, the time $\tau_{\max} = 1/\omega_{\max}$ (Table II), locating the maximum in the loss modulus (after correction for contributions of the transition zone to G''), is proportional to $M^{3.1}$ for the star polymers, a slightly weaker dependence than $M^{3.4}$ observed for the linear polymers. Thus, in the star polymers, the simple relation between τ_{\max} and η_0 is altered. A possible explanation is that the set of terminal relaxation mechanisms, characterizing the star when no enhancement of η_0 is observed, splits into two sets when the molecular weight becomes high. The longer time mechanism, perhaps associated with movements of the whole molecule, might increase exponentially with molecular weight.

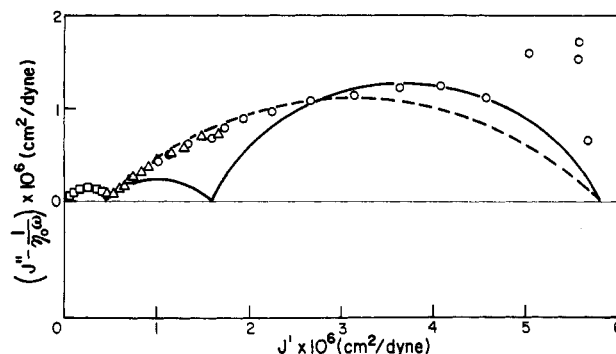


Figure 9. Cole-Cole plot for S181A. Experimental points: squares, 140 °C; triangles, 170 °C; circles, 200 °C. Full line: three arcs of a circle representing three retardation mechanisms with from left to right τ_t , τ_b , and τ_{enh} . Broken line: two retardation mechanisms τ_t and τ_p .

Relaxations involving smaller parts of the molecule, perhaps single arms of the star, might still be governed by the laws for linear entangled polymers.

To check this hypothesis more quantitatively, the data were analyzed in terms of the complex compliance.²¹ The components of complex compliance $J^*(\omega)$ were calculated from²

$$J'(\omega) = \frac{G'(\omega)}{[G'(\omega)]^2 + [G''(\omega)]^2} \quad (13a)$$

$$J''(\omega) = \frac{G''(\omega)}{[G'(\omega)]^2 + [G''(\omega)]^2} \quad (13b)$$

The complex compliance is then represented by

$$J^*(\omega) = J_g + \frac{1}{j\omega\eta_0} + J_r^*(\omega) \quad (14)$$

where J_g is the shear compliance of the glass, which is $\sim 10^{-10} \text{ cm}^2/\text{dyn}$ and negligible compared with the other terms. It was shown that the retardational compliance $J_r^*(\omega)$ can be expressed in terms of two groups of retardation mechanisms for linear polystyrene melts.²¹

$$J_r^*(\omega) = \frac{J_p}{1 + (j\omega\tau_p)^{1-\alpha}} + \frac{J_t}{1 + (j\omega\tau_t)^{1-\beta}} \quad (15)$$

J_p and J_t are the contributions to J_e^0 from the terminal and transition zones, respectively. The characteristic times for these contributions are τ_p and τ_t ; α and β are about 0.3 for high molecular weight linear polystyrenes with narrow molecular weight distributions.

If star polymers with enhanced viscosity have a new retardation mechanism at very long times, a third term in eq 15 would be required. Figure 9 shows a Cole-Cole plot for the data of four-star sample S181A. Three circular arcs are drawn through the data, representing three retardation mechanisms for which, at 170 °C, $J_t = 4.5 \times 10^{-7} \text{ cm}^2/\text{dyn}$, $\tau_t = 6.3 \times 10^{-4} \text{ s}$, $\beta = 0.3$; $J_b = 1.3 \times 10^{-6} \text{ cm}^2/\text{dyn}$, $\tau_b = 14.0 \text{ s}$, $\alpha = 0.34$; and for the term representing enhancement, $J_{\text{enh}} = 4 \times 10^{-6} \text{ cm}^2/\text{dyn}$, $\tau_{\text{enh}} = 690 \text{ s}$, $\gamma = 0.3$. Equation 15 with three terms and these nine constants was used to calculate $J_r'(\omega)$ and $J_r''(\omega)$. From $J_r'(\omega)$ and $J_r''(\omega)$ and eq 14, one obtains $J'(\omega)$ and $J''(\omega)$, and with eq 13, $G'(\omega)$ and $G''(\omega)$ can be obtained. These calculated values are compared with the experimental moduli in Figure 10.

The alternative representation of the terminal region of S181A by a single retardation mechanism is also shown in Figure 10. $J_p = 5.35 \times 10^{-6} \text{ cm}^2/\text{dyn}$, $\tau_p = 400 \text{ s}$, and $\alpha = 0.48$ were derived by replacing two circular arcs in Figure 9 by a single one. It can be seen that the two curves

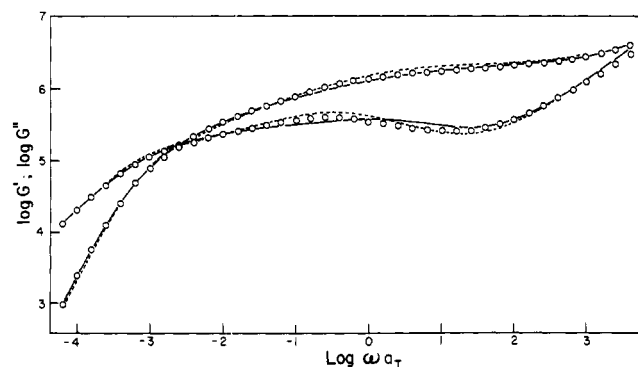


Figure 10. Comparison of experimental (circles) and calculated moduli-frequency curves of S181A: full line, model with three retardation mechanisms; dotted line, model with two retardation mechanisms.

approximate the experimental data with about equal accuracy. A similar observation was made in the analysis of G' and G'' data of comb-shaped polystyrenes whenever τ values became as close as τ_b and τ_{enh} .²⁸ A definitive test for an additional retardation mechanism in star polymers will apparently require higher molecular weight samples with still larger enhancement factors.

Acknowledgment. The authors wish to express their thanks to W. Rochefort, E. Menezes, and V. Raju, graduate students at Northwestern University, for help with various parts in this work. Use of the facilities of the Northwestern University Materials Research Center, supported by the National Science Foundation, is acknowledged with gratitude.

References and Notes

- (1) G. C. Berry and T. G. Fox, *Adv. Polym. Sci.*, **5**, 261 (1968).
- (2) J. D. Ferry, "Viscoelastic Properties of Polymers", 2nd ed., Wiley, New York, 1970.
- (3) W. W. Graessley, *Adv. Polym. Sci.*, **16**, 1 (1974).
- (4) P. E. Rouse, *J. Chem. Phys.*, **21**, 272 (1953).
- (5) J. S. Ham, *J. Chem. Phys.*, **26**, 625 (1957).
- (6) F. Bueche, *J. Chem. Phys.*, **40**, 484 (1964).
- (7) L. A. Utracki and J. Roovers, *Macromolecules*, **6**, 366 (1973).
- (8) J. Roovers and N. Hadjichristidis, *J. Polym. Sci.*, **12**, 2521 (1974).
- (9) H. Kajiura, Y. Ushiyama, T. Fujimoto, and M. Nagasawa, *Macromolecules*, **11**, 894 (1978).
- (10) T. G. Fox and V. R. Allen, *Polym. Prepr., Am. Chem. Soc., Div. Polym. Chem.*, **3**, 6 (1962); ONR, Technical Report, No. 10, Mellon Institute.
- (11) T. Masuda, Y. Ohta, and S. Onogi, *Macromolecules*, **4**, 763 (1971).
- (12) G. Kraus and J. T. Gruver, *J. Polym. Sci., Part A*, **3**, 105 (1965).
- (13) W. W. Graessley, T. Masuda, J. Roovers, and N. Hadjichristidis, *Macromolecules*, **9**, 127 (1976).
- (14) P. G. de Gennes, *J. Phys. (Paris)*, **36**, 1199 (1975).
- (15) J. Roovers and S. Bywater, *Macromolecules*, **5**, 384 (1972); **7**, 443 (1974).
- (16) L. A. Utracki and J. Roovers, *Macromolecules*, **6**, 373 (1973).
- (17) C. W. Macosko and W. M. Davis, *Rheol. Acta*, **13**, 814 (1974).
- (18) W. E. Rochefort, private communication.
- (19) J. Roovers and P. M. Toporowski, *J. Appl. Polym. Sci.*, **18**, 1685 (1974).
- (20) P. M. Toporowski and J. Roovers, *J. Polym. Sci., Polym. Chem. Ed.*, **14**, 2233 (1976).
- (21) G. Marin and W. W. Graessley, *Rheol. Acta*, **16**, 527 (1977).
- (22) N. J. Mills and A. Nevin, *J. Polym. Sci., Part A-2*, **9**, 267 (1971).
- (23) W. M. Prest Jr., *J. Polym. Sci., Part A-2*, **8**, 1897 (1970).
- (24) D. J. Plazek and V. M. O'Rourke, *J. Polym. Sci., Part A-2*, **9**, 209 (1971).
- (25) E. Riande, H. Markovitz, d. J. Plazek, and N. Ragupathi, *J. Polym. Sci., Polym. Symp. Ed.*, **50**, 405 (1975).
- (26) A. Rudin and K. K. Chee, *Macromolecules*, **6**, 613 (1973).
- (27) Reference 3, Table 5.4, p 64.
- (28) J. Roovers, to be published.

Specific Volumes of Styrene-Butadiene Block Copolymers

Sarah Martin Glass and Malcolm Dole*¹

Department of Chemistry, Baylor University, Waco, Texas 76703. Received May 31, 1979

ABSTRACT: The specific volumes at 25 °C of one AB and of two ABA block copolymers of butadiene (B) and styrene (A) were measured as were also the specific volumes of the polybutadiene and polystyrene homopolymers. Although the specific volumes of the block copolymers nearly follow an ideal additive law, the slight deviations in the direction of greater volume than expected can be explained on a statistical basis.

Block copolymers have considerable theoretical interest and industrial importance. Their synthesis and properties have been extensively reviewed.²⁻⁵ However, very little work has been devoted solely to studying the specific volumes of block copolymers. Renuncio and Prausnitz⁶ recently measured the specific volumes at 75 °C of some random and some block copolymers of butadiene (B) and styrene (A) and found within the accuracy of their measurements that the specific volume was a linear function of the weight percentage of styrene. Our data given below, which were taken at 25 °C, approximately confirm the linear relation, but the deviations are systematic and can be interpreted in a significant way.

This paper represents the beginning of a series of studies on block copolymers which will include measurements of hydrogen and deuterium gas solubilities in the solid copolymers so as to determine the free volume available to these gases (research already under way) and kinetic studies of free-radical decay in irradiated samples of the block copolymers.

Table I
Properties of Butadiene and Styrene Block Copolymers and Homopolymers (Polystyrene is Atactic Polystyrene)

structural type	wt fraction of styrene	% microstructure			$M_n^a \times 10^{-3}$
		cis	trans	vinyl	
B	0	40.0	52.0	8.0	150
ABA	0.212	27.7	55.1	17.2	164
ABA	0.418	25.8	62.5	11.7	258
AB	0.612	29.6	54.2	16.2	606
A	1.000				193

^a The number average molecular weights were determined by osmometry except for the AB block copolymer whose M_n value is a theoretical one calculated from the polymerization charge.

Experimental Section

Materials. The homopolymers and block copolymers studied and their properties are listed in Table I. They were prepared by R. A. Livigni of the General Tire and Rubber Co. and were sent to us along with the data of Table I courtesy of Dr. S. L.